

Highly anisotropic magnetic states of Co dimers bound to graphene-vacancies

Hem C. Kandpal, Klaus Koepernik, and Manuel Richter
IFW Dresden e.V., PO Box 270116, D-01171 Dresden, Germany
 (Dated: March 4, 2013)

The adsorption behavior and the magnetic states of cobalt atoms and dimers on single vacancies in a graphene sheet are investigated by means of relativistic density functional calculations. It is found that local magnetic moments are formed in both cases, despite strong chemical binding. Of particular interest are kinetically stable isomers with two cobalt atoms attached to the same side of the graphene sheet. Magnetic bi-stability with an anisotropy barrier of about 50 meV is possible in this geometry. The feasibility of its preparation is discussed.

PACS numbers: 81.05.ue, 75.30.Gw, 75.75.Lf, 31.15.es

Keywords: density functional theory, magnetic anisotropy of nanostructures, transition metals on graphene

Nanoscale magnets with large magnetic anisotropy (MA) are of interest both for fundamental research [1–3] and for technological applications [4, 5]. Experimental activities to produce such systems were hitherto mainly focused on one of two known routes, the chemical synthesis of single-molecule magnets (SMM) or the physical deposition of magnetic atoms or small clusters on metallic substrates. Both routes resulted in systems with maximum MA energies (MAE) somewhat below 10 meV per magnetic atom or per SMM: Single Co atoms deposited on a Pt(111) surface show an MAE of 9 meV per Co atom [1]; an anisotropy barrier of 7 meV was reported for a complex of the Mn_6 family of SMM [2].

Recently, the MA of four 3d transition metal dimers was predicted to be up to one order of magnitude larger than these figures [6, 7]. In the case of Co dimers, adsorption on pristine graphene does obviously not harm their magnetic properties. Their MAE has been estimated by density-functional (DF) calculations [8] to be of the order of 100 meV. This finding adds a new flavor to the remarkable features of graphene [9, 10] (G) which has been praised [11] for its electronic, mechanical, optical, and thermal properties.

Its structural robustness [11], impermeability [12], chemical tolerance [13], and reassemble properties [14] distinguish G as a salient substrate material. As such, it has been applied to adsorb metal atoms [15, 16] and clusters [17]. Several theoretical studies confirmed that magnetic moments are to be expected on transition metal atoms and dimers including cobalt adsorbed on G [18–21]. Thus, Co_2 -G seems to be suited for ultrahigh-density magnetic recording [8].

Unfortunately, the binding of transition metal atoms and dimers to pristine G is relatively weak. In the case of Co dimers, the DF binding energy amounts to about 0.7 eV. [8] However, a yet smaller activation energy of 0.24 eV (upper limit) for surface migration was measured for gold atoms on graphite [22] and migration barriers in the range of 0.01 to 0.8 eV were evaluated [18, 23] by DF calculations for transition metal adatoms on G. At room temperature, Co atoms are hence expected to float on the

carbon layer [23]. Indeed, STM images of Co atoms on pristine G were only obtained at 4.2 Kelvin [24], hitherto.

Defect structures of carbon are highly reactive. Thus, one possibility to bind transition metal atoms or dimers more strongly consists in a deliberate creation of structural defects, e.g. single vacancies with dangling bonds, in the G sheet before the adsorbate is deposited. An established experimental route to produce isolated vacancies in graphene-like systems is irradiation with low-energy Ar^+ ions [25]. After annealing, most defects produced in this way were found to be single vacancies [26].

For the case of Co atoms, a binding energy to a single vacancy in graphene (SVG) of about 8 eV was predicted [23], by far large enough to ensure stability at room temperature. Strong chemical binding, on the other hand, often spoils magnetism. In particular, orbital magnetism which is chiefly responsible for the MA is known to be quenched by hybridization and crystal fields. While the existence of spin magnetism was predicted for atomic impurities of several transition metals in G including Co-SVG [23, 27], we are not aware of related investigations concerning orbital magnetic properties. It is thus both demanding and interesting to find magnetic graphene-based nanostructures that are structurally stable on the one hand and show a large orbital moment or even a large MA on the other hand.

Here, we present Co_2 -SVG as an example of a nanostructure that possibly fulfills both contradicting requirements. The related system Co-SVG is demonstrated to be a counterexample where the strong binding suppresses the MA. As a specific intricacy, the desired large MA of Co_2 -SVG is not present in the ground state but in kinetically stable isomers which can be prepared in the most simple way by atom-wise deposition. The suggested preparation can be considered as a combination of the two known routes to produce nanomagnets with large MA, the chemical (SMM) and the physical (adsorbate deposition) one.

The DF calculations were performed with the all-electron full-potential local-orbital (FPLO) code [28], version 9.00-34. The exchange-correlation energy func-

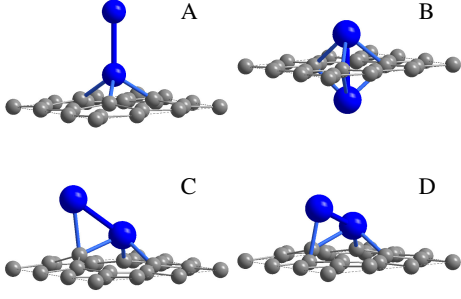


FIG. 1: (Color online) Four isomers (A)-(D) of $\text{Co}_2\text{-SVG}$ obtained by relaxation of five initial geometries [30]. Large blue spheres: cobalt atoms; small gray spheres: carbon atoms.

$\text{Co}_2\text{-SVG}$	(A0)	(AI)	(AII)	(B)	(C)	(D)
E_{tot} (eV)	0.9	1.0	1.2	0	1.1	1.4
μ_s (μ_B)	2.0	2.0	2.0	1.7	2.0	1.8
E_{spin} (eV)	0.7	0.8	1.0	0.1	0.5	0.1

TABLE I: Relative total energies, E_{tot} , and total spin moments, μ_s , of the structural isomers of $\text{Co}_2\text{-SVG}$, Fig. 1. E_{spin} denotes the stabilization energy of spin magnetism, i.e., the energy difference between non-magnetic and magnetic state. Structure (A) can be stabilized in three different electronic states: (A0), (AI), and (AII).

tional was evaluated using the standard parameterization [29] of the generalized gradient approximation (GGA). Orbital magnetic properties were calculated in a four-component fully relativistic mode. To obtain an upper estimate for the MAE [8], orbital polarization corrections [31] (OPC) were applied in some of the calculations. The technical parameters of the calculations are described in the Online Supplement [30].

Recent DF results indicate that *single* Co atoms on *pristine* G are magnetically bistable with an MAE-barrier in the 10-meV range [8]. Further, using GGA it has already been found that Co atoms bound to an SVG keep a spin moment of $1 \mu_B$, while Fe and Ni atoms become non-magnetic [23, 27]. These predictions tempted us to check the magnetic anisotropy of Co-SVG, before considering the more complex case of Co dimers. The values of spin moment, $\mu_s(\text{Co-SVG}) = 0.92 \mu_B$, energy needed for Co detachment, $E_{\text{Co-det}}(\text{Co-SVG}) = 8.0 \text{ eV}$, and Co-C bond length, $d^{\text{Co-C}}(\text{Co-SVG}) = 1.76 \text{ \AA}$, found in our calculations [30] confirm the available literature data [23, 27, 32]. By checking the orbital magnetic properties, we however find negligible magnitudes of the orbital moment, $\mu_l(\text{Co-SVG}) < 0.01 \mu_B$, and of the MAE ($< 0.1 \text{ meV}$) in both GGA and GGA+OPC approaches. Thus, we conclude that the orbital magnetism of *single* Co atoms is quenched by binding to an SVG.

There are several structures for the interaction of *two* Co atoms with SVG imaginable. We considered five

m	-2	-1	0	1	2
(A0)	0.0	0.9	0.1	0.9	1.0
(AI)	0.5	0.5	0.8	0.5	0.5
(AII)	0.5	0.9	0.1	0.9	0.5
(C)	0.6	0.5	0.8	0.4	0.6

TABLE II: Orbital-resolved occupation numbers of 3d spin-down states of r-Co for the three electronic isomers of the geometry (A) and for geometry (C). The quantum numbers m refer to real spherical harmonics.

initial geometries [30]. Relaxation of these geometries resulted in four (meta)stable structures, (A) to (D) in Fig. 1. In the case of (A), we found three different electronic isomers (A0), (AI), and (AII). They are distinguished by specific 3d-orbital occupations at the “remote” Co atom (r-Co) which is not directly bound to the vacancy. The relative total energies and the spin moments of all isomers are given in Tab. I, their structural details are compiled in the Online Supplement [30].

All identified $\text{Co}_2\text{-SVG}$ isomers are magnetic with spin $S = 1$. This is a notable difference to the $S = 2$ states of free Co dimers [6] and of $\text{Co}_2\text{-G}$ [8]. The lower spin state of $\text{Co}_2\text{-SVG}$ mirrors the stronger chemical bonding of Co at the vacancy compared to the pristine carbon hexagon.

Table II compiles the 3d spin-down orbital occupation numbers of r-Co for (A0-II). In all three isomers, the spin moment resides on r-Co and the Co atom at the vacancy (v-Co) is nearly spin-compensated. Thus, the spin-up channel of r-Co is almost completely occupied. State (A0) is lower in energy than (AI) and (AII), but its charge density lacks axial symmetry. Using a GGA+ U mode with $U, J \rightarrow 0$ we were able to stabilize all three states in a scalar relativistic GGA calculation for a free Co atom. The energy sequence is now (A0, free) - (AII, free) at 0.1 eV - (AI, free) at 0.2 eV. The correct atomic ground state has an axially symmetric charge density like (AI, free) or (AII, free), but unlike (A0, free). If spin-orbit interaction (s-o) is switched on, we find $L = 0$ for (A0, free), $L = 3$ for (AI, free), and $L = 2$ for (AII, free). Considering Hund’s second rule, the best GGA approximation to the atomic ground state is (AI, free), the second best is (AII, free). Both facts, its broken axial symmetry and its incompatibility with Hund’s second rule, lead us to disregard the state (A0, free) as unphysical. Its low energy is due to self-interaction of the non-spherical part of the charge density, as discussed earlier by Brooks *et al.* [34]. Bonding of the free Co atom to Co-SVG slightly shifts the energies of the three electronic isomers, but hardly changes their orbital occupations. We therefore exclude (A0) from the further discussion.

Structure (B), where the two Co atoms are located on opposite sides of the G plane, is the ground-state isomer. However, we will now provide arguments that it is

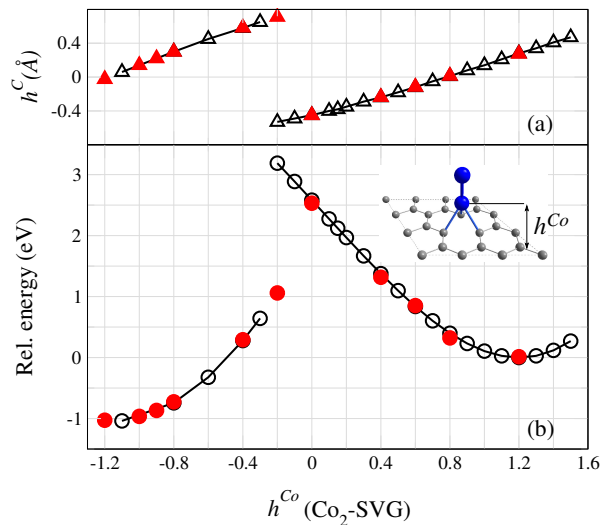


FIG. 2: (Color online) Diffusion barrier between Co₂-SVG(AI) and Co₂-SVG(B). The inset shows the considered structure. The height of the Co atom next to the vacancy, h^{Co} , was fixed (abscissa of the figure). Black (open) symbols: space group 156 (P3m1), red (full) symbols: space group 1 (P1). Relaxation was allowed for the height of the three neighboring carbon atoms, h^{C} of Panel (a), their lateral position, and the distance between the two Co atoms (not shown). Panel (b) displays the total energy relative to the energy of Co₂-SVG(AI). The two minima in the energy curves are related to the two isomers (AI) and (B), the diffusion barrier amounts to 2...2.5 eV, estimated by extrapolation of the left branch.

technically easier to produce a structure with both Co atoms on the same side of the carbon layer and that this situation is kinetically stable.

Deposition of small Co amounts on a graphene-like surface with beforehand-prepared single vacancies will yield Co-SVG under ambient conditions, since Co atoms are mobile on pristine surface areas. A fraction of the Co atoms may agglomerate [Co-G → G + hcp-Co], but the related energy gain per Co atom [30], $E_{\text{Co-agg}} = -4.4$ eV, has a smaller absolute value than the energy gained by binding to the SVG [Co-G + SVG → G + Co-SVG], $E_{\text{b}}(\text{Co} - \text{SVG}) = -6.8$ eV. We further note, that Co-SVG is expected to be stable against migration at room temperature. Related activation energies for Pt-SVG and Au-SVG were found to be close to 2.5 eV by high-temperature transmission electron microscopy [33].

If Co-deposition is continued after saturation of the vacancies, a large fraction of the mobile Co atoms will attach to Co-SVG and form Co₂-SVG(AI) or one of its quasi-degenerate isomers (AII) or (C). The reaction [Co-G + Co-SVG → G + Co₂-SVG(AI)] gains an energy [30] of $E_{\text{b}}(\text{Co}_2 - \text{SVG}) = -1.2$ eV. Agglomeration of the Co atoms with a gain of -4.4 eV would be energetically yet more favorable, but obviously the formation of Co₂-SVG is kinetically more likely at low deposition

orientation		(AI)	(AII)	(C)
001	$\mu_s(\text{v-Co})$	0.0	-0.1 (-0.1)	0.0 (0.0)
100	$\mu_s(\text{v-Co})$	0.0	-0.1 (-0.1)	0.0 (0.0)
001	$\mu_s(\text{r-Co})$	2.1	2.3 (2.3)	2.0 (2.0)
100	$\mu_s(\text{r-Co})$	2.1	2.3 (2.3)	2.0 (2.0)
001	$\mu_l(\text{r-Co})$	0.3	2.0 (2.1)	0.2 (2.2)
100	$\mu_l(\text{r-Co})$	0.2	0.2 (0.8)	0.2 (0.6)
MAE (meV)		0.1	63 (53)	0.6 (44)

TABLE III: Results from fully relativistic GGA calculations for Co₂-SVG(A) and Co₂-SVG(C). The notations 001 and 100 refer to magnetic moment orientations perpendicular and parallel to the C plane, respectively. Magnetic spin moments μ_s and orbital moments μ_l are projected on the cobalt atoms next to the vacancy (v-Co) and on the other Co atom (r-Co) and given in μ_{B} . The MAE is the difference between total energies obtained for the two chosen moment orientations, $\text{MAE} = E(100) - E(001)$, and refers to the whole structural unit with two Co atoms. The in-plane anisotropy is small and can be neglected. Results in parentheses refer to GGA+OPC calculations.

rates and sufficient supply of Co-SVG sites. The substrate temperature should be low enough to avoid detachment of Co from Co₂-SVG (below 300 K, estimated from $|E_{\text{b}}(\text{Co}_2 - \text{SVG})| = 1.2$ eV), but high enough to ensure mobility of the deposited Co atoms on G.

Finally, we check if Co₂-SVG(AI) is kinetically stable against diffusion of the Co atom next to the vacancy to the other side of the G sheet [Co₂-SVG(AI) → Co₂-SVG(B)]. Fig. 2 presents the geometry and the energy of structures along the diffusion path. We find an energy barrier of more than 2 eV, large enough to ensure stability beyond detachment of the upper Co atom. This large barrier arises from the fact that the Co atomic radius is much larger than the radius of the missing carbon atom. Thus, Pauli repulsion on the one hand and stiffness of the carbon plane on the other hand hinder the diffusion. *We conclude that preparation of Co₂-SVG with both Co atoms located at the same side of the C plane is possible and that this structure is stable up to about 300 K.*

Considering the size of the discussed self-energy error for systems containing almost free atoms, we are not able to judge if (AI), (AII), or (C) is the ground state isomer. We however tend to exclude geometry (D), which lies 0.4 eV above (AI), from the further discussion. We also note that the magnetic state of (AI), (AII), and (C) is more stable than that of the other isomers, cf. the spin stabilization energies in Tab. I.

We now turn the attention to orbital magnetic properties. Tab. III compiles results for the kinetically stable low-lying isomers. In the case of (AI), any self-consistent GGA+OPC calculation converged to the state (AII). This might be an indication that (AI) is not realized in nature. Most remarkably, the MAE of (AII) and of (C) in the GGA+OPC approach is predicted to be similarly

high as that of Co₂-G [8], though in the present case the Co dimer is much more tightly bound to the substrate and thus has a much better chance to be accessible to experimental realization.

Strong chemical bonding claims its price, though. The atomic-site projected magnetic moments of the Co atom next to the vacancy are almost completely quenched, Tab. III. However, large spin moments ($S = 1$) persist on r-Co due to the low coordination of this atom. For (AII) and for (C) in OPC, also the orbital moment is large, $L = 2$. Magnetic moment orientation perpendicular to the easy (001) axis quenches the orbital moment but requires a large energy, the MAE, which is related to the orbital moment reduction [35, 36].

Among the two Co atoms, a distribution of tasks takes place: v-Co atom is strongly bound to SVG and serves as an anchor for r-Co; the remote r-Co, on the other hand, preserves atomic-like properties and carries those electronic states which produce an ultimately high MAE. From this distribution of tasks it is clear that atoms of elements other than cobalt could be used as anchor atoms and/or remote atoms. Thus, Co₂-SVG is most likely only one example of a whole class of unknown highly anisotropic nanomagnets.

To summarize, we suggest that deposition of Co atoms on SVG can be used to prepare a structure with two Co atoms attached to each vacancy. We demonstrated its kinetic stability and found strong indications that it will show an exceptionally high MA. Single Co atoms on Pt also show large MA [1], but their technological use might be restricted by a high spin tunneling probability [3]. For the present system, the hybridization of the magnetically active atom with its surrounding is much smaller than in the case of a metallic substrate, since the chemical bonding is mediated by a single anchor atom. Thus, Co₂-SVG might even be of technological interest for magnetic data storage.

We finally note that Co₂-SVG should be considered as one didactic example of a whole class of possible structures, consisting of an organic substrate with dangling bonds and a few metal atoms. The “remote” atoms show strong orbital magnetism, while the “anchor” atoms mediate the bonding to the substrate. The production of such systems could make use of a self-assembling step: the saturation of the dangling bonds by anchor atoms.

Financially supported by DFG grant RI932/6-1.

[1] P. Gambardella, S. Rusponi, M. Veronese, S. S. Dhesi, C. Grazioli, A. Dallmeyer, I. Cabria, R. Zeller, P. H. Dederichs, K. Kern, et al., *Science* **300**, 1130 (2003).
 [2] C. J. Milios, A. Vinslava, W. Wernsdorfer, S. Moggach, S. Parsons, S. P. Perlepes, G. Christou, and E. K. Brechin, *J. Am. Chem. Soc.* **129**, 2754 (2007).

[3] T. Balashov, T. Schuh, A. F. Takács, A. Ernst, S. Ostannin, J. Henk, I. Mertig, P. Bruno, T. Miyamachi, S. Suga, et al., *Phys. Rev. Lett.* **102**, 257203 (2009).
 [4] T. Thomson, L. Abelman, and H. Groenland, *Magnetic Nanostructures in Modern Technology: Spintronics, Magnetic MEMS and Recording* (Springer, Heidelberg, 2008), chap. Magnetic data storage: Past present and future, pp. 237–306, NATO Science for Peace and Security Series B - Physics and Biophysics.
 [5] H. Stillrich, C. Menk, R. Frömter, and H. P. Oepen, *J. Appl. Phys.* **105**, 07C308 (2009).
 [6] T. O. Strandberg, C. M. Canali, and A. H. MacDonald, *Nature Materials* **6**, 648 (2007).
 [7] D. Fritsch, K. Koepnik, M. Richter, and H. Eschrig, *J. Comput. Chem.* **29**, 2210 (2008).
 [8] R. Xiao, D. Fritsch, M. D. Kuz'min, K. Koepnik, H. Eschrig, M. Richter, K. Vietze, and G. Seifert, *Phys. Rev. Lett.* **103**, 187201 (2009).
 [9] A. H. C. Neto, F. Guinea, N. M. R. Peres, K. S. Novoselov, and A. K. Geim, *Rev. Mod. Phys.* **81**, 109 (2009).
 [10] M. J. Allen, V. C. Tung, and R. B. Kaner, *Chem. Rev.* **110**, 132 (2010).
 [11] A. K. Geim, *Science* **324**, 1530 (2009).
 [12] J. S. Bunch, S. S. Verbridge, J. S. Alden, A. M. van der Zande, J. M. Parpia, H. G. Craighead, and P. L. McEuen, *Nano Letters* **8**, 2458 (2008).
 [13] J. Shen, Y. Hu, C. Li, C. Qin, and M. Ye, *Small* **5**, 82 (2009).
 [14] S.-M. Paek, E. Yoo, and I. Honma, *Nano Lett.* **9**, 72 (2009).
 [15] I. Gierz, C. Riedl, U. Starke, C. R. Ast, and K. Kern, *Nano Lett.* **8**, 4603 (2008).
 [16] C. G. Hwang, S. Y. Shin, S.-M. Choi, N. D. Kim, S. H. Uhm, H. S. Kim, C. C. Hwang, D. Y. Noh, S.-H. Jhi, and J. W. Chung, *Phys. Rev. B* **79**, 115439 (2009).
 [17] R. Muszynski, B. Seger, and P. V. Kamat, *J. Phys. Chem. C* **112**, 5263 (2008).
 [18] K. T. Chan, J. B. Neaton, and M. L. Cohen, *Phys. Rev. B* **77**, 235430 (2008).
 [19] H. Johll, H. C. Kang, and E. S. Tok, *Phys. Rev. B* **79**, 245416 (2009).
 [20] C. Cao, M. Wu, J. Jiang, and H.-P. Cheng, *Phys. Rev. B* **81**, 205424 (2010).
 [21] H. Zhang, C. Lazo, S. Blügel, S. Heinze, and Y. Mokrousov, *Phys. Rev. Lett.* **108**, 056802 (2012).
 [22] R. Anton and I. Scheidereit, *Phys. Rev. B* **58**, 13874 (1998).
 [23] A. V. Krasheninnikov, P. O. Lehtinen, A. S. Foster, P. Pyykkö, and R. M. Nieminen, *Phys. Rev. Lett.* **102**, 126807 (2009).
 [24] V. W. Brar, R. Decker, H.-M. Solowan, Y. Wang, L. Maserati, K. T. Chan, H. Lee, Ç. O. Girit, A. Zettl, S. G. Louie, et al., *Nature Physics* **7**, 43 (2010).
 [25] S. M. Lee, Y. H. Lee, Y. G. Hwang, J. R. Hahn, and H. Kang, *Phys. Rev. Lett.* **82**, 217 (1999).
 [26] M. M. Ugeda, I. Brihuega, F. Guinea, and J. M. Gómez-Rodríguez, *Phys. Rev. Lett.* **104**, 096804 (2010).
 [27] E. J. G. Santos, D. S.-Portal, and A. Ayuela, *Phys. Rev. B* **81**, 125433 (2010).
 [28] K. Koepnik and H. Eschrig, *Phys. Rev. B* **59**, 1743 (1999), URL <http://www.fplo.de/>.
 [29] J. P. Perdew, K. Burke, and M. Ernzerhof, *Phys. Rev. Lett.* **77**, 3865 (1996).

- [30] URL [onlinesupplement](#).
- [31] O. Eriksson, M. S. S. Brooks, and B. Johansson, Phys. Rev. B **41**, 7311 (1990).
- [32] D. W. Boukhvalov and M. I. Katsnelson, App. Phys. Lett. **95**, 023109 (2009).
- [33] Y. Gan, L. Sun, and F. Banhart, Small **4**, 587 (2008).
- [34] M. S. S. Brooks, O. Eriksson, J. M. Wills, and B. Johansson, Phys. Rev. Lett. **79**, 2546 (1997).
- [35] P. Bruno, Phys. Rev. B **39**, 865 (1989).
- [36] R. Xiao, D. Fritsch, M. D. Kuz'min, K. Koepernik, H. Eschrig, M. Richter, K. Vietze, and G. Seifert, Phys. Rev. B **82**, 205125 (2010).

Supplementary material

This Supplement reports technical details of the calculations, results of the optimization of geometry and/or spin state, definitions of reaction energies and convergence checks for the simulation cell size.

Technical details of the calculations

The convergence with respect to the k -space grid density was carefully checked. Using a linear tetrahedron method with Blöchl corrections, the final calculations were performed with $9 \times 9 \times 1$ k -points in the full Brillouin zone (geometry optimization) or with $30 \times 30 \times 1$ k -points (orbital magnetism). The basis set comprised Co (3s, 3p, 3d, 4s, 4p, 4d, 5s) and C (1s, 2s, 2p, 3s, 3p, 3d) states. The modified G sheet was modeled with a 3×3 supercell of fixed edge length 7.392 Å in the x - y plane and with 12 Å spacing along the z direction. Calculations with a 4×4 cell and with 16 Å spacing did not show any significant difference, see below.

Geometry optimization was carried out using forces evaluated in a scalar relativistic mode with a convergence criterion of 1 meV/Å. Fixed spin-moment calculations were employed to exclude the existence of spin states not found by the unrestricted self-consistent calculations.

Optimization of geometry and/or spin state

The geometry and/or the spin magnetic state of eight different systems were optimized with respect to the total GGA energy: a free Co atom, a free Co dimer (Co_2), bulk Co metal in the hexagonal close-packed structure (Co-hcp), a Co atom on pristine graphene (Co-G), a Co dimer on pristine graphene (Co_2 -G), graphene with a single vacancy (SVG), Co-SVG, and Co_2 -SVG with four identified structural isomers, called (A, B, C, D), see Fig. S1 and Fig. 1 of the main text. In the isomer Co_2 -SVG (B), the two Co atoms are located on opposite sides of the graphene sheet. Thus, this isomer is also referred to as Co-SVG-Co.

All graphene-derived systems were treated in a 3×3 structural unit cell. For comparison, the total energy of pristine graphene (G) is computed in a fixed geometry, according to the fixed unit cell size used in the other calculations. All energies and spin moments in Tabs. SI and SII refer to the considered structural unit, i.e., to 18 carbon atoms for G, to 18 carbon atoms and 1 (2) cobalt atom(s) for Co-G (Co_2 -G), to 17 carbon atoms for SVG, and to 17 carbon atoms and 1 (2) cobalt atom(s) for Co-SVG (Co_2 -SVG).

All calculations were performed with the code and settings defined in the main text, exceptions are mentioned in the column ‘remarks’. For Co atoms and dimers, the

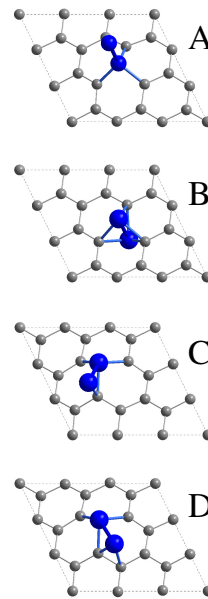


FIG. S1: Four isomers (A)-(D) of Co_2 -SVG obtained by relaxation of five initial geometries, see Fig. S2. Blue spheres denote cobalt atoms and gray spheres denote carbon atoms. Fig. 1 of the main text shows the same structures in a different view.

molecular mode with free boundary conditions was applied. All other calculations were performed with three-dimensional periodic boundary conditions.

In the atomic calculations, the 3d and 4s states turn out to be degenerate. The lowest GGA energy corresponds to a configuration $3d^{7.6}4s^{1.4}$. Spin-orbit coupling has a stronger influence on the atomic total energies than on the total energies of atoms in a cluster, molecule, or bulk compound. We included related data obtained in fully relativistic mode for the Co atom and the Co dimer in Tab. SI but used the values obtained in scalar relativistic mode to calculate binding energies for the sake of comparability with other published (scalar relativistic) DF energies [23]. Binding energies related to atomic Co would have to be corrected by the amount $E(\text{Co} - \text{atom}) - E_r(\text{Co} - \text{atom}) = 0.08$ eV. The correction related to a Co dimer amounts to less than 0.02 eV, see Tab. SI.

Fig. S2 shows the five chosen initial structures used to identify isomers of Co_2 -SVG by structural relaxation. The initial SVG structure was always prepared by removing one carbon atom from the pristine graphene sheet without relaxation. The two Co atoms were initially placed in the following positions to form the initial structures (I) to (V):

- (I) both above the vacancy site at heights of 1.5 and 3.5 Å;
- (II) above and below the vacancy site at heights of 1.5 and -1.5 Å;

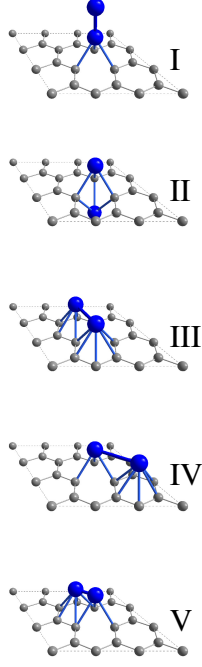


FIG. S2: Five chosen initial geometries (I)-(V) of $\text{Co}_2\text{-SVG}$.

(III) above the centers of two pentagons next to the vacancy at the same height of 1.5 Å;
 (IV) above the vacancy site and above the center of a neighboring hexagon at the same height of 1.5 Å;
 (V) above the vacancy site and above the center of a pentagon next to the vacancy at the same height of 1.5 Å.

The initial geometries for Co-G and Co-SVG were prepared by positioning the cobalt atom above the center of a hexagon at a height of 1.5 Å and above the vacancy site at a height of 1.5 Å, respectively. In the case of $\text{Co}_2\text{-G}$, the Co atoms were placed above the center of a hexagon at heights of 1.5 and 3.5 Å.

A summary of results for all optimized geometries is given in Tabs. SI and SII. The calculated atomic distances d and heights h in Tabs. SI and SII refer to nearest neighbor distances and to the distances to the x - y plane, respectively. In particular, $d^{\text{C-C}}$ denote the distances between pairs of the three carbon atoms next to the vacancy, h^{C} is the displacement of these atoms from the x - y plane, $d^{\text{Co-C}}$ are the distances between the cobalt atom next to the vacancy and the related carbon atoms, and h^{Co} is the distance of the cobalt atom next to the vacancy from the x - y plane.

A notable structural deformation was found at the vacancy site for the $\text{Co}_2\text{-SVG}$ -isomers (A), (C), and (D), where the three carbon atoms next to the vacancy are pulled out up to 0.6 Å from the graphene plane.

In the case of structure (A) we found three electronic isomers. Isomer (A0) was obtained if the calculation was

performed in space group 1, the other two, (AI) and (AII), in space group 156, using different starting conditions.

Reaction energies

We define reaction energies of the following processes, referred to in the main text:

Energy needed for the detachment of Co atoms from SVG (reaction $\text{Co-SVG} \rightarrow \text{Co-atom} + \text{SVG}$),

$$\begin{aligned} E_{\text{Co-det}}(\text{Co} - \text{SVG}) &= \\ E(\text{Co} - \text{atom}) + E(\text{SVG}) - \\ &\quad - E(\text{Co} - \text{SVG}) = 7.96 \text{ eV} . \end{aligned} \quad (1)$$

Energy gained by agglomeration of Co atoms on graphene (reaction $\text{Co-G} \rightarrow \text{G} + \text{hcp-Co}$),

$$\begin{aligned} E_{\text{Co-agg}} &= \\ E(\text{G}) + E(\text{Co} - \text{hcp}) - \\ &\quad - E(\text{Co} - \text{G}) = -4.43 \text{ eV} . \end{aligned} \quad (2)$$

Energy gained by binding of Co atoms on graphene to SVG (reaction $\text{Co-G} + \text{SVG} \rightarrow \text{G} + \text{Co-SVG}$),

$$\begin{aligned} E_{\text{b}}(\text{Co} - \text{SVG}) &= \\ E(\text{G}) + E(\text{Co} - \text{SVG}) - \\ &\quad - E(\text{Co} - \text{G}) - E(\text{SVG}) = -6.76 \text{ eV} . \end{aligned} \quad (3)$$

Energy gained by binding of Co atoms on graphene to Co-SVG. For reasons explained in the main text, we take isomer (AI) as reference (reaction $\text{Co-G} + \text{Co-SVG} \rightarrow \text{G} + \text{Co}_2\text{-SVG(AI)}$),

$$\begin{aligned} E_{\text{b}}(\text{Co}_2 - \text{SVG}) &= \\ E(\text{G}) + E(\text{Co}_2 - \text{SVG(AI)}) - \\ &\quad - E(\text{Co} - \text{G}) - E(\text{Co} - \text{SVG}) = -1.15 \text{ eV} . \end{aligned} \quad (4)$$

Convergence of the simulation cell

We checked the magnetic moment and binding energy of Co-SVG with a 4×4 supercell and found that the ground state has a magnetic moment of $0.99 \mu_{\text{B}}$. The Co-detachment energy of this structure amounts to 7.99 eV. These values are almost the same as those obtained with a 3×3 supercell, $0.92 \mu_{\text{B}}$ and 7.96 eV.

In the case of SVG, the 3×3 supercell yields equal distances between the carbon atoms next to the vacancy and a vacancy formation energy,

$$\begin{aligned} E_{\text{vac}}(3 \times 3) &= \\ E(\text{SVG}, 3 \times 3) - E(\text{G}, 3 \times 3) \cdot 17/18 &= 7.95 \text{ eV} . \end{aligned} \quad (5)$$

If a 4×4 supercell is used, the so-called 5-9 structure is obtained where two of the carbon atoms next to the vacancy form a loose pair. Accordingly, the vacancy formation energy is about 0.1 eV smaller than in the former case,

$$E_{\text{vac}}(4 \times 4) = E(\text{SVG}, 4 \times 4) - E(\text{G}, 4 \times 4) \cdot 31/32 = 7.84 \text{ eV} . \quad (6)$$

The dependence of $E(\text{SVG})$ on the size of the simulation cell is compensated by an opposite dependence of $E(\text{Co} - \text{SVG})$. Thus, $E_{\text{Co-det}}(\text{Co} - \text{SVG})$ is almost independent of the cell size. We conclude that the reaction energies are reliable at a level of 0.1 eV, if 3×3 supercells are used.

system	space group	geometry parameters [Å]	total energy [eV]	spin moment [μ_B]	remarks
Co atom			$E = -37916.34$	3.00	scalar relativistic
Co atom			$E_r = -37916.42$	3.00	fully relativistic
Co ₂		$d^{\text{Co-Co}} = 1.989$	$E = -75836.44$	4.03	scalar relativistic
Co ₂		$d_r^{\text{Co-Co}} = 1.989$	$E_r = -75836.45$	4.03	fully relativistic, distance fixed
Co-hcp	194 (P6 ₃ /mmc)	$a = 2.5071$ $c = 4.0695$	$E = -37921.97$	1.62	experimental geometry k -mesh $96 \times 96 \times 60$ scalar relativistic
G	156 (P3m1)	$d_G^{\text{C-C}} = 1.4226$	$E = -18663.46$	0	experimental geometry k -mesh $60 \times 60 \times 1$ scalar relativistic

TABLE SI: Compilation of reference energies and other properties of Co atoms, Co dimers, bulk Co, and pristine graphene.

system	space group	geometry parameters [Å]	total energy [eV]	spin moment [μ_B]
Co-G	183 (P6mm)	$d^{\text{Co-C}} = 2.111$ $h^{\text{Co}} = 1.560$	$E = -56581.00$	1.06
Co ₂ -G	183 (P6mm)	$d^{\text{Co-Co}} = 2.054$ $d^{\text{Co-C}} = 2.250$ $h^{\text{Co}} = 1.743$	$E = -94500.57$	4.06
SVG	1 (P1)	$d^{\text{C-C}} = 2.545, 2.546, 2.545$ $h^{\text{C}} = 0$	$E = -17618.65$	1.04
Co-SVG	1 (P1)	$d^{\text{Co-C}} = 1.762, 1.762, 1.762$ $h^{\text{Co}} = 1.144$	$E = -55542.96$	0.92
Co ₂ -SVG (A0)	1 (P1)	$d^{\text{Co-Co}} = 2.250$ $d^{\text{Co-C}} = 1.763, 1.763, 1.763$ $h^{\text{Co}} = 1.195$ $h^{\text{C}} = 0.270, 0.275, 0.275$	$E = -93461.76$	2.00
Co ₂ -SVG (AI)	156(P3m1)	$d^{\text{Co-Co}} = 2.280$ $d^{\text{Co-C}} = 1.764$ $h^{\text{Co}} = 1.200$ $h^{\text{C}} = 0.275$	$E = -93461.65$	2.00
Co ₂ -SVG (AII)	156(P3m1)	$d^{\text{Co-Co}} = 2.246$ $d^{\text{Co-C}} = 1.764$ $h^{\text{Co}} = 1.200$ $h^{\text{C}} = 0.276$	$E = -93461.48$	2.00
Co ₂ -SVG (B)	1 (P1)	$d^{\text{Co-C}} = 1.876, 1.876, 1.876$ $h^{\text{Co}} = 1.171$ $h^{\text{C}} = 0.0, 0.0, 0.0$	$E = -93462.68$	1.71
Co ₂ -SVG (C)	1 (P1)	$d^{\text{Co-Co}} = 2.303$ $d^{\text{Co-C}} = 1.760, 1.760, 1.777$ $h^{\text{Co}} = 1.238, 2.566$ $h^{\text{C}} = 0.232, 0.231, 0.586$	$E = -93461.54$	2.00
Co ₂ -SVG (D)	1 (P1)	$d^{\text{Co-Co}} = 2.338$ $d^{\text{Co-C}} = 1.760, 1.784, 1.763$ $h^{\text{Co}} = 1.240, 1.986$ $h^{\text{C}} = 0.154, 0.312, 0.445$	$E = -93461.27$	1.75

TABLE SII: Compilation of geometries, total energies, and spin moments of Co-G, Co₂-G, SVG, Co-SVG, and Co₂-SVG structures, obtained in scalar relativistic mode.